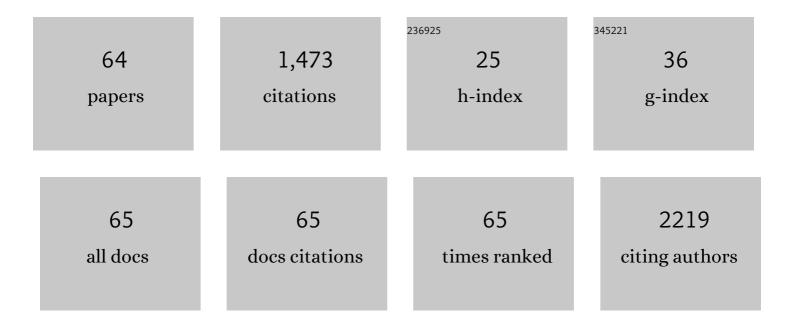
List of Publications by Year in descending order

Source: https://exaly.com/author-pdf/1970230/publications.pdf Version: 2024-02-01



#	Article	IF	CITATIONS
1	Crosstalk between Yeast Cell Plasma Membrane Ergosterol Content and Cell Wall Stiffness under Acetic Acid Stress Involving Pdr18. Journal of Fungi (Basel, Switzerland), 2022, 8, 103.	3.5	15
2	The BASHY Platform Enables the Assembly of a Fluorescent Bortezomib–GV1001 Conjugate. ACS Medicinal Chemistry Letters, 2022, 13, 128-133.	2.8	4
3	Improved Parameterization of Phosphatidylinositide Lipid Headgroups for the Martini 3 Coarse-Grain Force Field. Journal of Chemical Theory and Computation, 2022, 18, 357-373.	5.3	24
4	Disclosing azole resistance mechanisms in resistant <i>Candida glabrata</i> strains encoding wild-type or gain-of-function <i>CgPDR1</i> alleles through comparative genomics and transcriptomics. G3: Genes, Genomes, Genetics, 2022, 12, .	1.8	5
5	Impact of Ca2+-Induced PI(4,5)P2 Clusters on PH-YFP Organization and Protein-Protein Interactions. Biomolecules, 2022, 12, 912.	4.0	0
6	Yeast adaptive response to acetic acid stress involves structural alterations and increased stiffness of the cell wall. Scientific Reports, 2021, 11, 12652.	3.3	25
7	The Azurin-Derived Peptide CT-p19LC Exhibits Membrane-Active Properties and Induces Cancer Cell Death. Biomedicines, 2021, 9, 1194.	3.2	6
8	Quantitative FRET Microscopy Reveals a Crucial Role of Cytoskeleton in Promoting PI(4,5)P2 Confinement. International Journal of Molecular Sciences, 2021, 22, 11727.	4.1	1
9	Acyl-chain saturation regulates the order of phosphatidylinositol 4,5-bisphosphate nanodomains. Communications Chemistry, 2021, 4, .	4.5	4
10	Silica nanoparticles with thermally activated delayed fluorescence for live cell imaging. Materials Science and Engineering C, 2020, 109, 110528.	7.3	23
11	Structure and Lateral Organization of Phosphatidylinositol 4,5-bisphosphate. Molecules, 2020, 25, 3885.	3.8	13
12	Engineering Boron Hot Spots for the Site‣elective Installation of Iminoboronates on Peptide Chains. Chemistry - A European Journal, 2020, 26, 15226-15231.	3.3	8
13	Förster Resonance Energy Transfer as a Tool for Quantification of Protein–Lipid Selectivity. Methods in Molecular Biology, 2019, 2003, 369-382.	0.9	1
14	The mechanism of action of pepR, a viral-derived peptide, against Staphylococcus aureus biofilms. Journal of Antimicrobial Chemotherapy, 2019, 74, 2617-2625.	3.0	23
15	SEDS–bPBP pairs direct lateral and septal peptidoglycan synthesis in Staphylococcus aureus. Nature Microbiology, 2019, 4, 1368-1377.	13.3	77
16	Measuring the Impact of Bile Acids on the Membrane Order of Primary Hepatocytes and Isolated Mitochondria by Fluorescence Imaging and Spectroscopy. Methods in Molecular Biology, 2019, 1981, 99-115.	0.9	1
17	Biophysical study of human induced Pluripotent Stem Cell-Derived cardiomyocyte structural maturation during long-term culture. Biochemical and Biophysical Research Communications, 2018, 499, 611-617.	2.1	35
18	Pdr18 is involved in yeast response to acetic acid stress counteracting the decrease of plasma membrane ergosterol content and order. Scientific Reports, 2018, 8, 7860.	3.3	54

#	Article	IF	CITATIONS
19	Azurin interaction with the lipid raft components ganglioside GM-1 and caveolin-1 increases membrane fluidity and sensitivity to anti-cancer drugs. Cell Cycle, 2018, 17, 1649-1666.	2.6	24
20	The combination of block copolymers and phospholipids to form giant hybrid unilamellar vesicles (CHUVs) does not systematically lead to "intermediate―membrane properties. Soft Matter, 2018, 14, 6476-6484.	2.7	20
21	<i>Staphylococcus aureus</i> haem biosynthesis and acquisition pathways are linked through haem monooxygenase IsdG. Molecular Microbiology, 2018, 109, 385-400.	2.5	18
22	Mixing Block Copolymers with Phospholipids at the Nanoscale: From Hybrid Polymer/Lipid Wormlike Micelles to Vesicles Presenting Lipid Nanodomains. Langmuir, 2017, 33, 1705-1715.	3.5	75
23	A Case of Selfâ€Organization in Highly Emissive Eu <sup>III</sup> Ionic Liquids. European Journal of Inorganic Chemistry, 2017, 2017, 3429-3434.	2.0	10
24	Modulation of phase separation at the micron scale and nanoscale in giant polymer/lipid hybrid unilamellar vesicles (GHUVs). Soft Matter, 2017, 13, 627-637.	2.7	57
25	Membrane Order Is a Key Regulator of Divalent Cation-Induced Clustering of PI(3,5)P <sub>2</sub> and PI(4,5)P <sub>2</sub> . Langmuir, 2017, 33, 12463-12477.	3.5	13
26	Membrane properties of giant polymer and lipid vesicles obtained by electroformation and pva gel-assisted hydration methods. Colloids and Surfaces A: Physicochemical and Engineering Aspects, 2017, 533, 347-353.	4.7	38
27	Accurate quantification of inter-domain partition coefficients in GUVs exhibiting lipid phase coexistence. RSC Advances, 2016, 6, 66641-66649.	3.6	5
28	Modulation of membrane properties of lung cancer cells by azurin enhances the sensitivity to EGFR-targeted therapy and decreased β1 integrin-mediated adhesion. Cell Cycle, 2016, 15, 1415-1424.	2.6	33
29	Characterization of a Squaraine/Chitosan System for Photodynamic Therapy of Cancer. Journal of Physical Chemistry B, 2016, 120, 1212-1220.	2.6	27
30	The Cytotoxic Bile Acid DCA Modulates Apoptotic Signalling through Alteration of Mitochondrial Membrane Properties. Biophysical Journal, 2015, 108, 242a.	0.5	1
31	Phase Separation and Nanodomain Formation in Hybrid Polymer/Lipid Vesicles. ACS Macro Letters, 2015, 4, 182-186.	4.8	69
32	Electrostatically driven lipid–protein interaction: Answers from FRET. Biochimica Et Biophysica Acta - Biomembranes, 2015, 1848, 1837-1848.	2.6	13
33	Deoxycholic acid modulates cell death signaling through changes in mitochondrial membrane properties. Journal of Lipid Research, 2015, 56, 2158-2171.	4.2	36
34	The Tyrosine Kinase BceF and the Phosphotyrosine Phosphatase BceD of Burkholderia contaminans Are Required for Efficient Invasion and Epithelial Disruption of a Cystic Fibrosis Lung Epithelial Cell Line. Infection and Immunity, 2015, 83, 812-821.	2.2	18
35	NIR and visible perylenediimide-silica nanoparticles for laser scanning bioimaging. Dyes and Pigments, 2014, 110, 227-234.	3.7	28
36	Ca2+ induces PI(4,5)P2 clusters on lipid bilayers at physiological PI(4,5)P2 and Ca2+ concentrations. Biochimica Et Biophysica Acta - Biomembranes, 2014, 1838, 822-830.	2.6	47

#	Article	IF	CITATIONS
37	Electrostatically driven lipid–lysozyme mixed fibers display a multilamellar structure without amyloid features. Soft Matter, 2014, 10, 840-850.	2.7	7
38	Role of calcium in membrane interactions by PI(4,5)P2-binding proteins. Biochemical Society Transactions, 2014, 42, 1441-1446.	3.4	16
39	Quantitative Evaluation of DNA Dissociation from Liposome Carriers and DNA Escape from Endosomes During Lipid-Mediated Gene Delivery. Human Gene Therapy Methods, 2014, 25, 303-313.	2.1	10
40	P116 INTERACTION OF APOPTOTIC AND CYTOPROTECTIVE BILE ACIDS WITH BIOMEMBRANES. Journal of Hepatology, 2014, 60, S105.	3.7	0
41	Characterization of BCAM0224, a Multifunctional Trimeric Autotransporter from the Human Pathogen Burkholderia cenocepacia. Journal of Bacteriology, 2014, 196, 1968-1979.	2.2	20
42	A combined fluorescence spectroscopy, confocal and 2-photon microscopy approach to re-evaluate the properties of sphingolipid domains. Biochimica Et Biophysica Acta - Biomembranes, 2013, 1828, 2099-2110.	2.6	38
43	The Apoptotic Bile Acid DCA has Preference for Association to Liquid Disordered Lipid Domains and Inhibits the Rigidifying Effect of Cholesterol in Membranes. Biophysical Journal, 2013, 104, 586a.	0.5	0
44	Physiological Calcium Concentrations Induce PI(4,5)P2 Clustering: PI(4,5)P2 as a Lipidic Calcium Sensor. Biophysical Journal, 2013, 104, 372a.	0.5	0
45	Förster Resonance Energy Transfer as a Tool for Quantification of Protein–Lipid Selectivity. Methods in Molecular Biology, 2013, 974, 219-232.	0.9	0
46	High performance NIR fluorescent silica nanoparticles for bioimaging. RSC Advances, 2013, 3, 9171.	3.6	29
47	Cytotoxic bile acids, but not cytoprotective species, inhibit the ordering effect of cholesterol in model membranes at physiologically active concentrations. Biochimica Et Biophysica Acta - Biomembranes, 2013, 1828, 2152-2163.	2.6	36
48	New Visible and NIR Highly Photostable Fluorescent Silica Nanoparticles for Laser Scanning Imaging Applications. Microscopy and Microanalysis, 2013, 19, 105-106.	0.4	2
49	Comparative Transcriptomic Analysis of the Burkholderia cepacia Tyrosine Kinase bceF Mutant Reveals a Role in Tolerance to Stress, Biofilm Formation, and Virulence. Applied and Environmental Microbiology, 2013, 79, 3009-3020.	3.1	45
50	Intrinsically Fluorescent Silica Nanocontainers: A Promising Theranostic Platform. Microscopy and Microanalysis, 2013, 19, 1216-1221.	0.4	19
51	Reorganization of lipid domain distribution in giant unilamellar vesicles upon immobilization with different membrane tethers. Biochimica Et Biophysica Acta - Biomembranes, 2012, 1818, 2605-2615.	2.6	38
52	High Affinity Immobilization of Giant Unilamellar Vesicles (GUVs) Induces Redistribution of Lipid Domains. Biophysical Journal, 2012, 102, 295a.	0.5	0
53	Advanced FRET Methodologies: Protein–Lipid Selectivity Detection and Quantification. Advances in Experimental Medicine and Biology, 2012, 749, 171-185.	1.6	1
54	Quantification of protein–lipid selectivity using FRET. European Biophysics Journal, 2010, 39, 565-578.	2.2	40

#	Article	IF	CITATIONS
55	Membrane microheterogeneity: Förster resonance energy transfer characterization of lateral membrane domains. European Biophysics Journal, 2010, 39, 589-607.	2.2	33
56	Quantitative Analysis of Domain Formation after Snare Mediated Fusion of Synaptic Vesicles. Biophysical Journal, 2010, 98, 678a.	0.5	0
57	Role of Helix 0 of the N-BAR Domain in Membrane Curvature Generation. Biophysical Journal, 2008, 94, 3065-3073.	0.5	58
58	Effects of fluorescent probe NBD-PC on the structure, dynamics and phase transition of DPPC. A molecular dynamics and differential scanning calorimetry study. Biochimica Et Biophysica Acta - Biomembranes, 2008, 1778, 491-501.	2.6	58
59	Ciprofloxacin interactions with bacterial protein OmpF: Modelling of FRET from a multi-tryptophan protein trimer. Biochimica Et Biophysica Acta - Biomembranes, 2007, 1768, 2822-2830.	2.6	33
60	Interaction of the Indole Class of Vacuolar H+-ATPase Inhibitors with Lipid Bilayersâ€. Biochemistry, 2006, 45, 5271-5279.	2.5	5
61	Binding assays of inhibitors towards selected V-ATPase domains. Biochimica Et Biophysica Acta - Biomembranes, 2006, 1758, 1777-1786.	2.6	13
62	Absence of clustering of phosphatidylinositol-(4,5)-bisphosphate in fluid phosphatidylcholine. Journal of Lipid Research, 2006, 47, 1521-1525.	4.2	37
63	Quantification of Protein-Lipid Selectivity using FRET: Application to the M13 Major Coat Protein. Biophysical Journal, 2004, 87, 344-352.	0.5	42
64	Dependence of M13 Major Coat Protein Oligomerization and Lateral Segregation on Bilayer Composition. Biophysical Journal, 2003, 85, 2430-2441.	0.5	42